

NASA MEMO 2-24-59A

LIBRARY  
Engineering Library  
NASA

SEP 4 1959

*Handwritten scribble*

*Handwritten scribble*

MEMORANDUM

THE EFFECT OF MOMENT-OF-AREA-RULE MODIFICATIONS ON THE  
DRAG, LIFT, AND PITCHING-MOMENT CHARACTERISTICS OF AN  
UNSWEPT ASPECT-RATIO-6 WING AND BODY COMBINATION

By Robert R. Dickey

Ames Research Center  
Moffett Field, Calif.

Engineering Library

NATIONAL AERONAUTICS AND  
SPACE ADMINISTRATION

WASHINGTON  
March 1959

1431



---

MEMORANDUM 2-24-59A

---

THE EFFECT OF MOMENT-OF-AREA-RULE MODIFICATIONS ON THE  
DRAG, LIFT, AND PITCHING-MOMENT CHARACTERISTICS OF AN  
UNSWEPT ASPECT-RATIO-6 WING AND BODY COMBINATION\*

By Robert R. Dickey

SUMMARY

An experimental investigation was conducted to determine the effect of moment-of-area-rule modifications on the drag, lift, and pitching-moment characteristics of a wing-body combination with a relatively high aspect-ratio unswept wing. The basic configuration consisted of an aspect-ratio-6 wing with a sharp leading edge and a thickness ratio of 0.06 mounted on a cut-off Sears-Haack body. The model with full moment-of-area-rule modifications had four contoured pods mounted on the wing and indentations in the body to improve the longitudinal distributions of area and moments of area. Also investigated were modifications employing pods and indentations that were only half the size of the full modifications and modifications with partial body indentations. The models were tested at angles of attack from  $-2^{\circ}$  to  $+12^{\circ}$  at Mach numbers from 0.6 to 1.4.

In general, the moment-of-area-rule modifications had a large effect on the drag characteristics of the models but only a small effect on their lift and pitching-moment characteristics. The modifications provided substantial reductions in the zero-lift drag at transonic and low supersonic speeds, but at subsonic speeds the drag was increased. Near Mach number 1.0, the model with full modification provided the greatest reduction in drag, but at the highest test Mach numbers the half modification gave the largest drag reduction. In general, the percent reductions of zero-lift drag obtained with the aspect-ratio-6 wing were as great or greater than those previously obtained with aspect-ratio-3 wings. The effect of the modifications on the drag due to lift was small except at Mach numbers below 0.9 where the modified models had higher drag-rise factors. Above Mach number 0.9, the modified models had higher lift-drag ratios than the basic model. The modified models also had higher lift curve slopes and generally were slightly more stable than the basic configuration.

---

\*Title, Unclassified

---

## INTRODUCTION

The moment-of-area-rule method for reducing the wave drag of wing-body combinations over a range of transonic and low supersonic Mach numbers was introduced in reference 1. In general, the moment-of-area rule indicates that the wave drag depends only on the longitudinal distributions of the area and moments of area taken about the vertical plane of symmetry, and that reductions in wave drag can be obtained if the fineness ratio and smoothness of these distributions are increased. It is shown in reference 1 that as the speed is increased above Mach number 1.0, successively higher order moment distributions become important in determining the wave drag of a configuration. Thus, at sonic speed, the wave drag depends only on the distribution of the cross-sectional or zero moment of area; whereas, at Mach numbers slightly above 1.0, the distribution of the second moment of area, as well as the cross-sectional area, becomes important. At still higher Mach numbers, the zero, second, and fourth moment distributions must be considered. It can also be shown from the drag equations of reference 1 that the higher order moment distributions become important as the aspect ratio increases.

Previous moment-of-area-rule investigations have been concerned with reducing the zero-lift wave drag of relatively low-aspect-ratio wing-body combinations near a Mach number of 1.0 by improving the distributions of area and second moment of area (see, e.g., refs. 1, 2, and 3). The purpose of the present investigation was to determine the effects of applying moment-of-area-rule modifications to a configuration with a wing of relatively high aspect ratio. Of primary interest were the drag reductions provided at lifting conditions as well as at zero lift and the effects of the modifications on the lift and pitching-moment characteristics.

To accomplish the foregoing objective, models of a wing-body combination with an aspect-ratio-6 unswept wing were tested with and without moment-of-area-rule modifications. The longitudinal distributions of the fourth moment of area as well as the cross-sectional area and the second moment of area were considered in the design of the modifications. The moment distributions were arbitrarily limited to the fourth power in order to simplify the design calculations. In addition to the configurations with complete moment-of-area-rule modifications, models were tested with modifications that were only one-half the size required for minimum drag near Mach number 1.0. It was reasoned that although such a design would sacrifice some drag reduction capability near Mach number 1.0, increased drag reductions would result at the higher Mach numbers because the average distribution of the projected area intercepted by the Mach planes would more nearly approximate the average distribution desirable for low drag at supersonic Mach numbers, as given in reference 4. Both the full moment-of-area-rule modification and the half moment-of-area-rule modification were also tested with partial body indentations that did not compensate for the added volume of the wing pcds. Although this type of

modification would not be expected to be as effective as a full indentation, it could be used to advantage in cases where the space requirements in a fuselage would prohibit the use of the full indentation.

The lift, drag, and pitching moment of the basic and modified models were measured at angles of attack from  $-2^\circ$  to  $+12^\circ$  over a Mach number range of 0.6 to 1.4. A constant Reynolds number of 0.8 million based on the mean aerodynamic chord of the wing was maintained throughout the test program.

#### NOTATION

A	aspect ratio
$C_D$	drag coefficient based on wing area
$C_{D_f}$	friction-drag coefficient
$C_{D_0}$	drag coefficient at zero lift
$C_{D_w}$	wave-drag coefficient, $C_{D_0} - C_{D_f}$
$\Delta C_{D_w}$	incremental wave-drag coefficient, $C_{D_w}$ of total configuration minus $C_{D_w}$ of basic body alone
$C_L$	lift coefficient based on wing area
$C_{L_\alpha}$	lift curve slope at $\alpha = 0$
$C_m$	pitching-moment coefficient referred to quarter-chord point of mean aerodynamic chord
$\bar{c}$	mean aerodynamic chord
$\frac{dC_D}{dC_L^2}$	drag-rise factor
$\frac{dC_m}{dC_L}$	slope of pitching-moment curve at $C_L = 0$
$\frac{L}{D}$	lift-drag ratio
$\left(\frac{L}{D}\right)_{\max}$	maximum lift-drag ratio
M	Mach number

R	Reynolds number
S	wing area
$\alpha$	angle of attack, deg
$\beta$	speed parameter, $\sqrt{M^2 - 1}$
$\lambda$	taper ratio of wing

## APPARATUS

The investigation was conducted in the Ames 2- by 2-foot transonic wind tunnel. This tunnel is of the closed-circuit, variable-pressure type and is equipped with a flexible nozzle and ventilated test section which permits continuous choke-free operation from 0 to 1.4 Mach number. A complete description of the wind tunnel may be found in reference 5. The models were mounted in the wind tunnel on a sting-supported internal strain-gage balance.

The five models described below were tested during this investigation:

1. Basic model (fig. 1(a)): The basic or unmodified configuration consisted of an aspect-ratio-6 unswept wing with an NACA 0006-05 airfoil section mounted on a cut-off Sears-Haack body.

2. Moment-of-area-rule model (fig. 1(b)): The model with the full moment-of-area-rule modifications prescribed in reference 1 had four contoured pods mounted on the wing and indentations in the body that compensated for the added volume of the wing pods as well as for part of the wing volume.

3. Moment-of-area-rule model with partial body indentation (fig. 1(b)): This model was identical to the fully modified model described above except that the body was not indented to compensate for the added volume of the wing pods.

4. Half moment-of-area-rule model (fig. 1(c)): The model with half-size modifications had wing pods and indentations for the wing that were only one-half the size prescribed in reference 1. The body was indented to compensate for the total volume of the half-size pods.

5. Half moment-of-area-rule model with partial body indentation (fig. 1(c)): This model was identical to the model with half-size moment-of-area-rule modifications described above except that the body was not indented to compensate for the added volume of the wing pods.

Before they were indented, the bodies of all models except that of the fully modified moment-of-area-rule model were the same size. The total volumes of the various configurations were therefore dependent on the amount of indentation in the body and on the size of the pods. The model with full moment-of-area-rule modification and complete body indentation utilized a body of slightly larger diameter than the other models so that its total volume was equal to that of the model which had the moment-of-area-rule modification with partial body indentation. These two models had a total volume 7 percent greater than that of the basic model. The volume of the model with half-size modifications and partial body indentations was 2 percent greater than that of the basic model, and with complete body indentations was 3 percent less than the basic model.

The effect of the various modifications on the longitudinal distributions of cross-sectional area is shown in figure 2. It may be seen that only the fully modified moment-of-area-rule model had an area distribution without protuberances. The half-size modifications eliminated only part of the bump caused by the wing, and the partial indentations did not compensate for the added cross-sectional area of the pods.

The longitudinal distributions of the second moment of area and of the fourth moment of area are shown in figures 3 and 4, respectively. The moments of area contributed by the body are small compared to those of the wing and pods and therefore have been neglected; consequently, the moment distributions show no effect of the various body indentations. It may be seen that the addition of the contoured pods increased the fineness ratio of the moment distributions without increasing their peak values.

#### TESTS AND DATA REDUCTION

The lift, drag, and pitching moment of the models were measured at angles of attack from  $-2^{\circ}$  to  $12^{\circ}$  at Mach numbers from 0.8 to 1.4. The zero-lift drag of the models was measured over a Mach number range of 0.6 to 1.4. A constant Reynolds number of 0.8 million based on the mean aerodynamic chord of the wing was maintained at all Mach numbers by varying the tunnel stagnation pressure. In order to assure a turbulent boundary layer over the entire surface of the models and thus permit the evaluation of friction drag with a minimum degree of uncertainty, the transition point of the boundary layer was fixed by carborundum strips placed near the leading edge of the wings and on the noses of the bodies and pods. The additional wave drag caused by the carborundum is believed to be small and should not affect the relative drag levels of the various configurations.

The measured drag of all models was adjusted to correspond to a condition of free-stream static pressure acting at the blunt base of the bodies and therefore all drag coefficients presented in this report represent the foredrag of the models. No corrections were applied to the data for wall-interference effects since the results of reference 6 indicate that for wing-body models of the size employed during the present tests (blockage ratios of approximately 0.6 percent) the interference effects would be small. Corrections for air-stream angularity and longitudinal pressure gradient were found to be small and have been neglected.

In addition to the small systematic errors which may be introduced because the corrections discussed above are neglected, the test data are subject to certain random errors of measurement. The random uncertainties of the test data at three Mach numbers and two angles of attack are listed in the following table:

	M = 0.6		M = 1.0		M = 1.4	
	$\alpha = 0^\circ$	$\alpha = 6^\circ$	$\alpha = 0^\circ$	$\alpha = 6^\circ$	$\alpha = 0^\circ$	$\alpha = 6^\circ$
M	$\pm 0.002$					
$\alpha$	$\pm .02^\circ$	$\pm .03^\circ$	$\pm .02^\circ$	$\pm .03^\circ$	$\pm .02^\circ$	$\pm .03^\circ$
$C_L$	$\pm .005$	$\pm .007$	$\pm .004$	$\pm .005$	$\pm .004$	$\pm .005$
$C_D$	$\pm .0003$	$\pm .0005$	$\pm .0003$	$\pm .0010$	$\pm .0003$	$\pm .0006$
$C_m$	$\pm .004$	$\pm .006$	$\pm .003$	$\pm .005$	$\pm .003$	$\pm .004$

## RESULTS AND DISCUSSION

The basic data for the unmodified and modified models are shown in figures 5 through 7 for several representative Mach numbers.

### Drag at Zero Lift

The zero-lift drag coefficients of the basic wing-body model, the modified models, and the basic body alone are shown plotted versus Mach number in figure 8. It may be seen that the modifications provided substantial drag reductions over most of the transonic and supersonic speed range investigated. The model with full moment-of-area-rule modifications had the lowest drag near Mach number 1.0, and the model with half modifications had the lowest drag at the higher supersonic Mach numbers. Although the models with partial indentations in the body also provided drag reductions over most of the transonic and supersonic speed range, in general, the reductions were not as large as those provided by the

corresponding modification with complete body indentation. Because of the additional surface area of the pods, the modified models had greater friction drag and therefore greater total drag than the basic model at subsonic speeds. However, at a Reynolds number representative of a full-scale airplane, the increased friction drag caused by the addition of pods would be less than that indicated by these low Reynolds number wind-tunnel tests. The solid symbols shown in figure 8 represent the test data adjusted to a Reynolds number of 30 million. The adjusted drag values shown for a Reynolds number of 30 million were obtained by reducing the friction drag measured at a Reynolds number of 0.8 million by the ratio of the corresponding Schoenherr friction coefficients given in reference 7. It was assumed that at a Mach number of 0.6 the measured fore-drag was entirely due to skin friction and that the variation of friction drag with Mach number was that given in reference 8 for a turbulent boundary layer.

The variation of wave-drag coefficient with Mach number for the various models is shown in figure 9. Wave drag was obtained by subtracting the friction drag, which was computed as described above, from the total zero-lift fore-drag. In the transonic speed range, all of the modifications provided large wave-drag reductions. The wave drag of the model with full moment-of-area-rule modifications was only 23 percent of that of the basic model at Mach number 1.0. The reductions in wave drag provided by the modifications became less as the Mach number increased, and at the highest test Mach number ( $M = 1.4$ ) the full moment-of-area rule and the moment-of-area rule with partial indentation in the body resulted in slightly higher wave drags than that of the basic configuration.

Since the moment-of-area rule attempts to minimize the additional wave drag caused by the addition of a wing to a body, it is necessary to isolate this part of the drag in order to determine how much of the drag caused by the wing was eliminated by the various modifications. This incremental wave drag (obtained by subtracting the wave drag of the basic body from the wave drag of the complete configurations) for the basic and modified models is shown in figure 10. At Mach number 1.0, the full moment-of-area-rule modifications were successful in eliminating 84 percent of the drag caused by the basic wing. At Mach number 1.4, however, this modification resulted in an increase of approximately 23 percent. The half moment-of-area-rule modifications, on the other hand, eliminated 60 percent of the drag caused by the basic wing at Mach number 1.0 and 11 percent at Mach number 1.4.

The effect of including the higher order moments of area in the design of the modification is shown in figure 11, wherein, the incremental wave-drag reductions obtained for the present quadripod design (moments up to and including the fourth moment) are compared to those obtained in references 1 and 3 for bipod designs (moments up to and including the second moment). Because the data were obtained from models of different aspect ratio, the results are plotted on a reduced aspect-ratio basis.

It is apparent that the modifications that considered the fourth moment-of-area distributions extended the wave-drag reductions to much higher values of  $\beta A$  than those that did not. It also appears that wave-drag reductions could be extended over a still higher  $\beta A$  range by considering the sixth or higher moment-of-area distributions.

It may be noted in figure 11 that at  $\beta A = 0$  ( $M = 1.0$ ) the drag reduction obtained with the fully modified aspect-ratio-6 wing was greater than that obtained with the aspect-ratio-3 unswept wing of reference 3. This difference is not explained by the theory of reference 1 since both models were modified to have the same shape of cross-sectional area distribution.

#### Drag at Lifting Conditions

The drag at lift coefficients of 0.2, 0.4, and 0.6 is shown in figure 12 for the basic model and the models with full and half moment-of-area-rule modifications. The results, in general, are similar to those at zero lift and indicate that the reductions in transonic drag provided by the moment-of-area-rule modifications are not limited to the zero-lift case but extend through a wide range of lifting conditions. Further evidence of this is shown in figure 13 where the lift-drag ratios of the basic and modified configurations are plotted versus lift coefficient for a subsonic, a transonic, and a supersonic Mach number.

In figure 14, the drag-rise factor and the maximum lift-drag ratio are plotted versus Mach number. As can be seen, the drag-rise factor was not appreciably changed by the moment-of-area-rule modifications except at Mach numbers below 0.9. The modifications did, however, have a considerable effect on the maximum lift-drag ratios. At subsonic speeds, the models with moment-of-area-rule modifications had lower maximum lift-drag ratios than the basic model, but at Mach numbers above 0.88 the modifications generally resulted in higher maximum lift-drag ratios. The largest increase occurred near Mach number 1.0 where the model with full moment-of-area-rule modifications had a maximum lift-drag ratio 38 percent greater than the basic model. Because of the higher friction-drag coefficients at low Reynolds numbers, the values of the lift-drag ratios obtained from these wind-tunnel tests are considerably lower than could be obtained at higher Reynolds numbers. An indication of the maximum lift-drag ratios that might be expected at a Reynolds number representative of a full-scale airplane is shown by the solid symbols in figure 14. To obtain these values, the measured drag of the models was adjusted to a Reynolds number of 30 million.

## Lift and Pitching-Moment Characteristics

The effect of the moment-of-area-rule modification on the lift characteristics of the configuration was in general beneficial (fig. 5). The lift curve slopes measured at  $\alpha = 0^\circ$  are plotted versus Mach number in figure 15. As can be seen, the modified models had greater lift curve slopes than the basic model. It can also be seen from figure 5 ( $C_L$  vs.  $\alpha$ ) that at subsonic speeds the modified models did not have the abrupt stall characteristics displayed by the basic model.

At supersonic speeds the modified models were more stable (see fig. 7). On the other hand, the basic model had slightly less variation of pitching-moment curve slope with Mach number, as can be seen from figure 15.

## CONCLUSIONS

An experimental wind-tunnel investigation was performed to determine the effect of moment-of-area-rule modifications on the drag, lift, and pitching-moment characteristics of a relatively high aspect-ratio wing-body combination. The results obtained from tests with an aspect-ratio-6 unswept wing indicate the following:

1. The minimum drag of a wing-body combination with a relatively high aspect-ratio wing was substantially reduced in the transonic and low supersonic speed range by means of moment-of-area-rule modifications which improved the distributions of the area and the second and fourth moments of area. However, the modifications resulted in increased drag at subsonic speeds.
2. The drag reductions provided by the moment-of-area-rule modifications were maintained throughout the normal range of lift coefficients; consequently, the modified models had higher lift-drag ratios at transonic and low supersonic speeds.
3. Near Mach number 1.0, the full moment-of-area-rule design resulted in the lowest drag, but at higher speeds ( $M = 1.06$  to  $1.40$ ) a design employing half-size modifications had the lowest drag. Partial modifications which did not indent the body to compensate for cross-sectional area of the pods generally resulted in smaller drag reductions.
4. The moment-of-area-rule modifications had no detrimental effect on the lift or pitching-moment characteristics. In general, the modified models had higher lift curve slopes and were slightly more stable than the basic model.

Ames Research Center  
National Aeronautics and Space Administration  
Moffett Field, Calif., Nov. 26, 1958

## REFERENCES

1. Baldwin, Barrett S., Jr., and Dickey, Robert R.: Application of Wing-Body Theory to Drag Reduction at Low Supersonic Speeds. NACA RM A54J19, 1955.
2. Levy, Lionel L., Jr., and Dickey, Robert R.: External-Store Drag Reduction at Transonic and Low Supersonic Mach Numbers by Application of Baldwin's Moment-of-Area Rule. NACA RM A55L14a, 1956.
3. Dickey, Robert R.: The Effect of Moment-of-Area-Rule Modifications on the Zero-Lift Drag of Three Wing-Body Combinations. NACA RM A58A31, 1958.
4. Jones, Robert T.: Theory of Wing-Body Drag at Supersonic Speeds. NACA Rep. 1284, 1956. (Supersedes NACA RM A53H18a)
5. Spiegel, Joseph M., and Lawrence, Leslie F.: A Description of the Ames 2- by 2-Foot Transonic Wind Tunnel and Preliminary Evaluation of Wall Interference. NACA RM A55I21, 1955.
6. Stivers, Louis S., Jr., and Lippmann, Garth W.: Effects of Fixing Boundary-Layer Transition for an Unswept-Wing Model and an Evaluation of Porous Tunnel-Wall Interference for Mach Numbers From 0.60 to 1.40. NACA TN 4228, 1958.
7. Locke, F. W. S., Jr.: Recommended Definition of Turbulent Friction in Incompressible Fluids. Navy, Bu. of Aero., Res. Div., DR Rep. No. 1415, June 1952.
8. Chapman, Dean R., and Kester, Robert H.: Turbulent Boundary-Layer and Skin-Friction Measurements in Axial Flow Along Cylinders at Mach Numbers Between 0.5 and 3.6. NACA TN 3097, 1954.

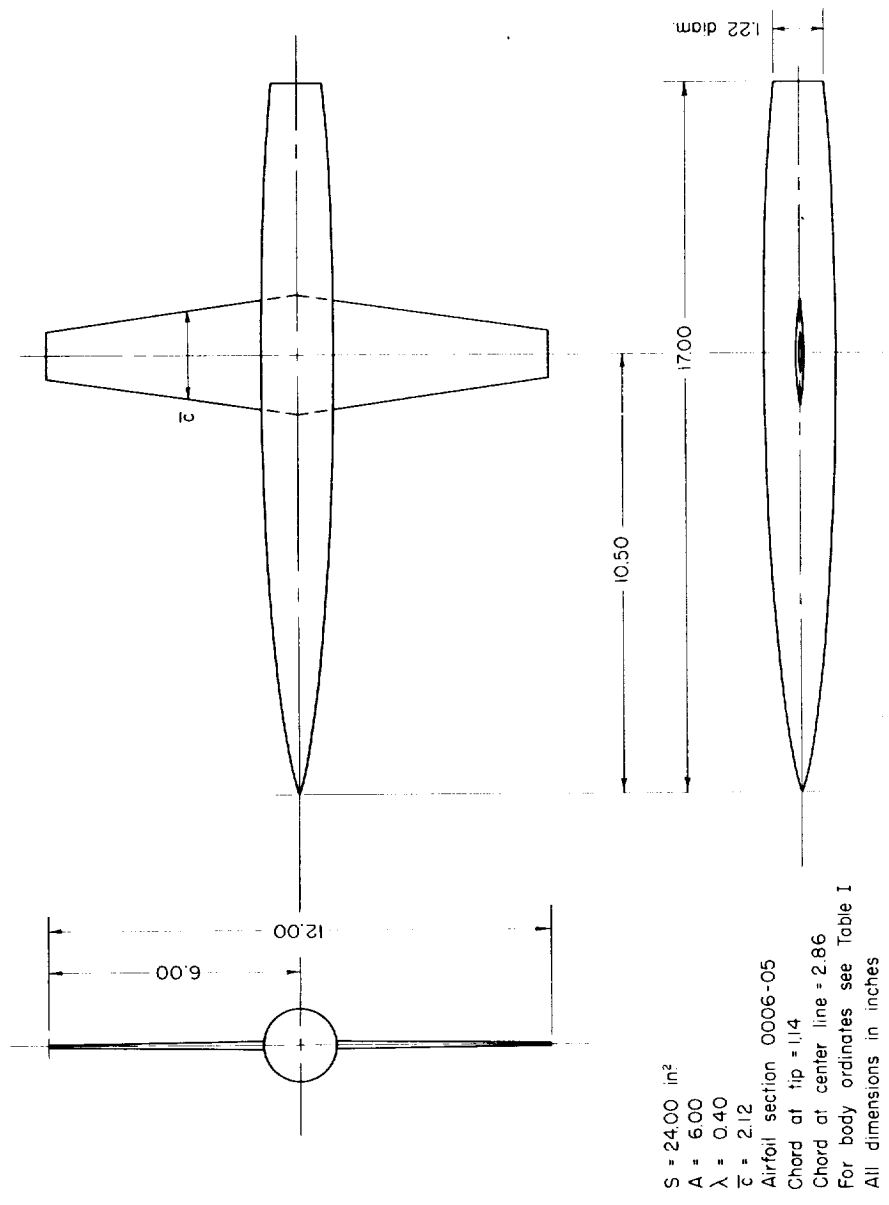
TABLE I.- BODY COORDINATES

Body station, in.	Body radius, in.				
	Basic	Moment-of-area rule		Half moment-of-area rule	
		Complete body indentation	Partial body indentation	Complete body indentation	Partial body indentation
0	0	0	0	0	0
.5	.147	.158	.147	.147	.147
1.0	.242	.257	.242	.242	.242
1.5	.323	.345	.323	.323	.323
2.0	.394	.420	.394	.394	.394
2.5	.457	.487	.457	.457	.457
3.0	.512	.546	.512	.512	.512
3.5	.562	.600	.562	.562	.562
4.0	.610	.649	.610	.610	.610
4.5	.651	.694	.651	.651	.651
5.0	.687	.733	.687	.687	.687
5.5	.721	.769	.721	.721	.721
6.0	.751	.801	.751	.751	.751
6.5	.778	.829	.778	.778	.778
7.0	.801	.842	.801	.801	.801
7.5	.820	.843	.820	.820	.820
8.0	.836	.838	.836	.833	.836
8.5	.851	.822	.851	.832	.851
9.0	.862	.800	.862	.821	.862
9.5	.870	.756	.846	.794	.858
10.0	.874	.716	.829	.770	.851
10.5	.875	.704	.823	.760	.850
11.0	.874	.716	.829	.770	.851
11.5	.870	.756	.846	.794	.857
12.0	.862	.800	.862	.821	.862
12.5	.851	.822	.851	.832	.851
13.0	.836	.838	.836	.833	.836
14.0	.801	.842	.801	.801	.801
15.0	.751	.801	.751	.751	.751
16.0	.687	.733	.687	.687	.687
17.0	.610	.649	.610	.610	.610

TABLE II.- POD COORDINATES

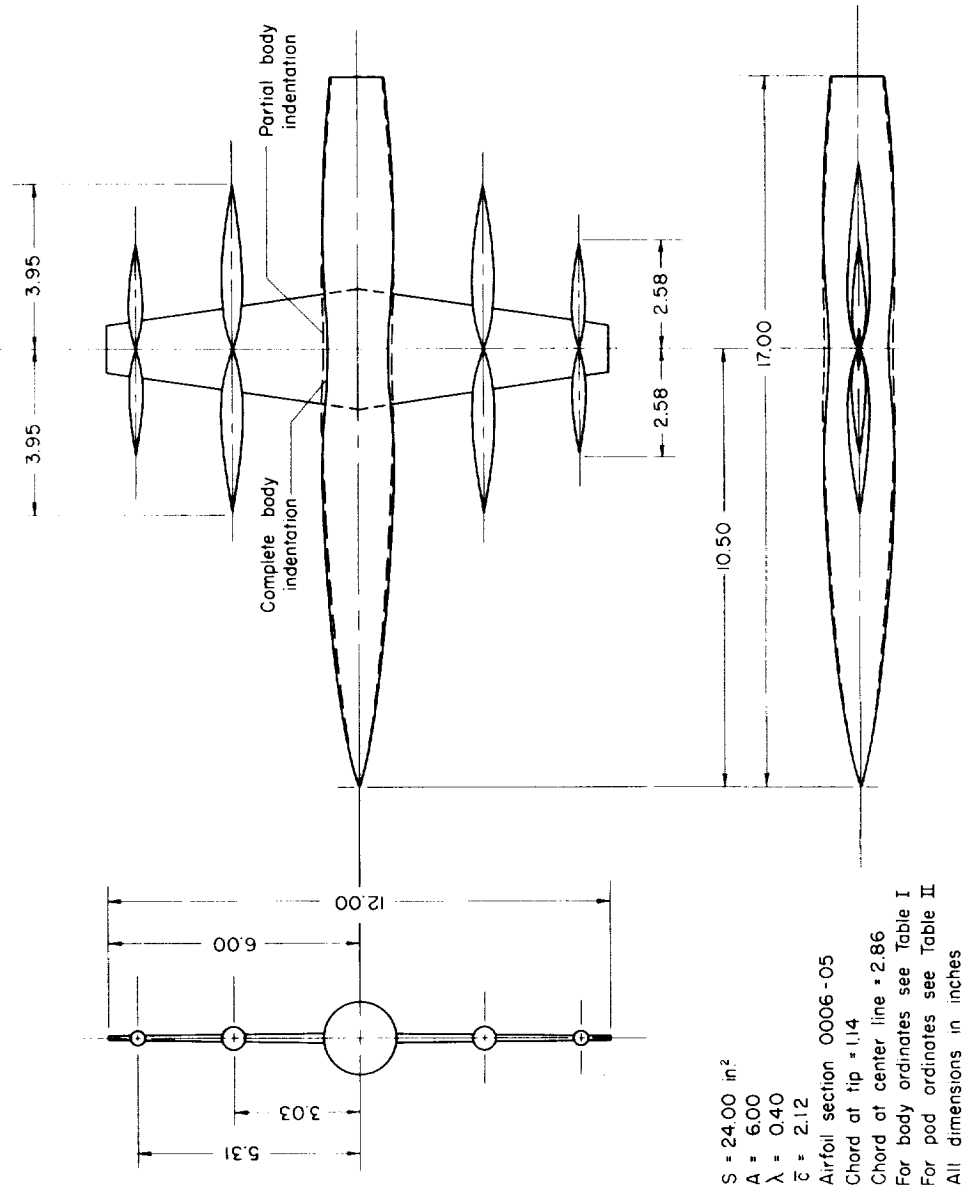
Pod station, <sup>1</sup> in.	Pod radius, in.			
	Moment-of-area rule		Half moment-of-area rule	
	Inboard pod	Outboard pod	Inboard pod	Outboard pod
0	0.060	0.040	0.060	0.040
.25	.103	.090	.084	.070
.50	.161	.155	.118	.105
.75	.238	.192	.168	.126
1.00	.286	.184	.190	.113
1.25	.292	.170	.187	.092
1.50	.281	.152	.173	.064
1.75	.268	.129	.153	.022
1.828	---	---	---	0
2.00	.253	.104	.130	
2.25	.235	.072	.102	
2.50	.215	.026	.067	
2.585	---	0	---	
2.75	.192		.014	
2.792	---		0	
3.00	.166			
3.25	.135			
3.50	.100			
3.75	.057			
3.95	0			

<sup>1</sup>Measured from midpoint of pod.



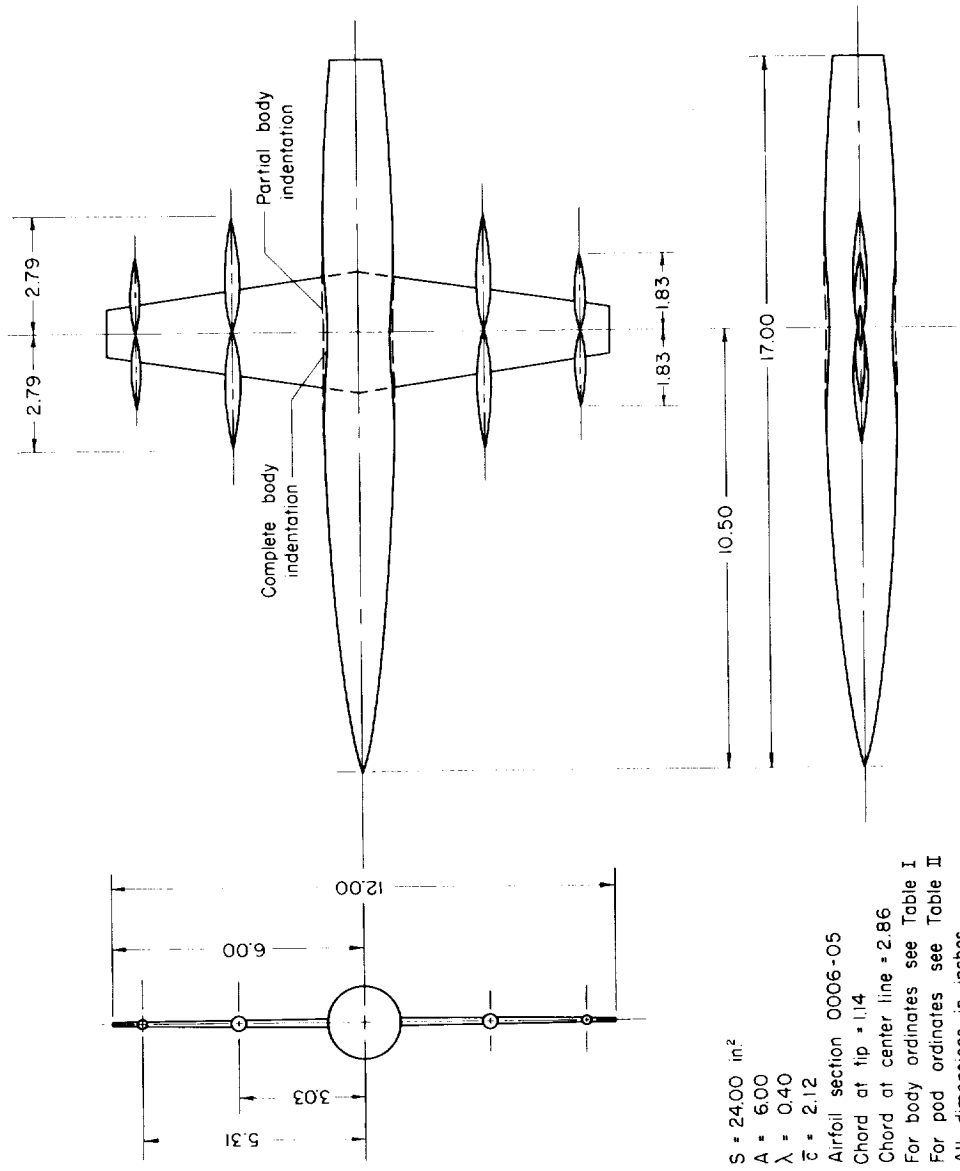
(a) Basic model.

Figure 1.- Dimensions and general arrangement of models.



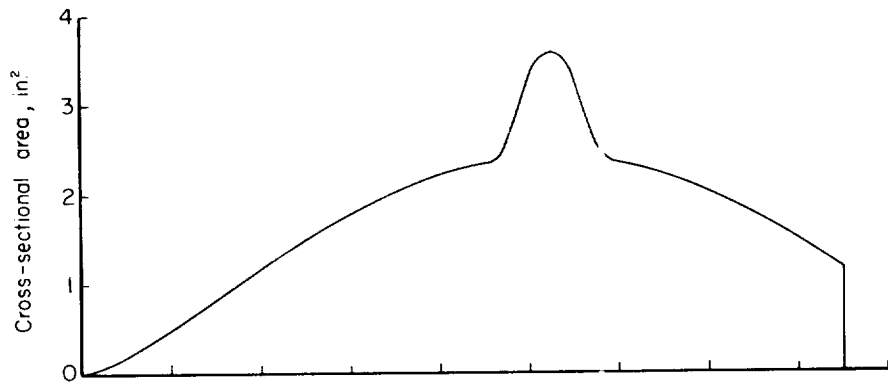
(b) Moment-of-area-rule modification.

Figure 1.- Continued.

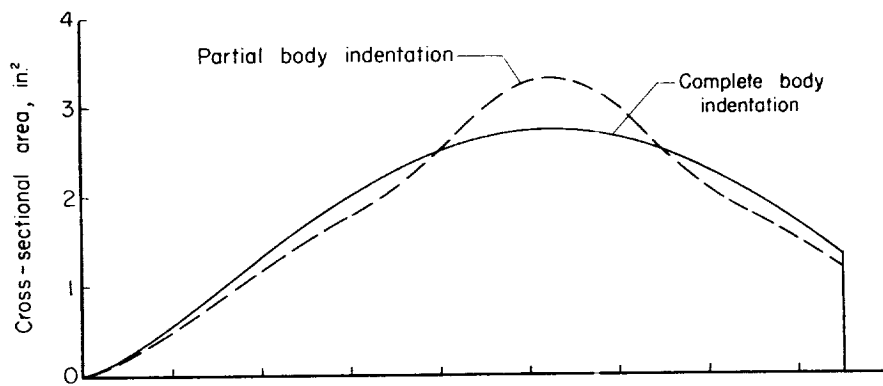


(c) Half moment-of-area-rule modification.

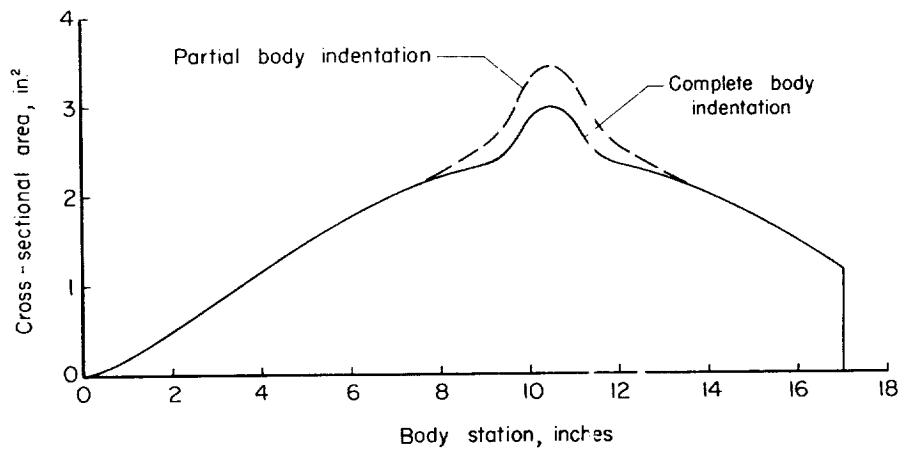
Figure 1.- Concluded.



(a) Basic wing-body combination.

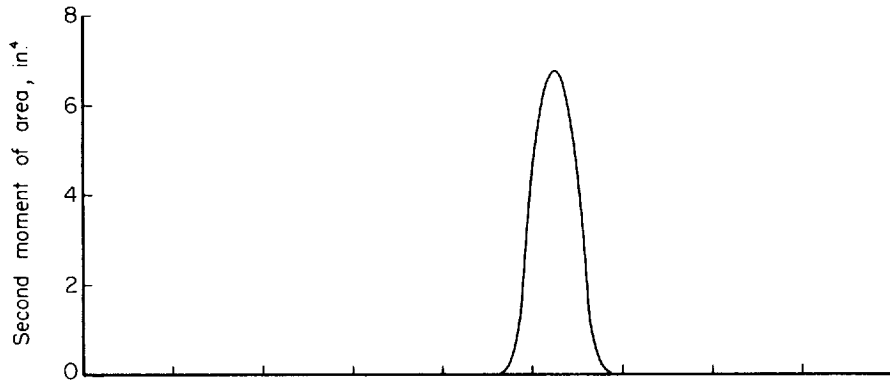


(b) Moment-of-area-rule modification.

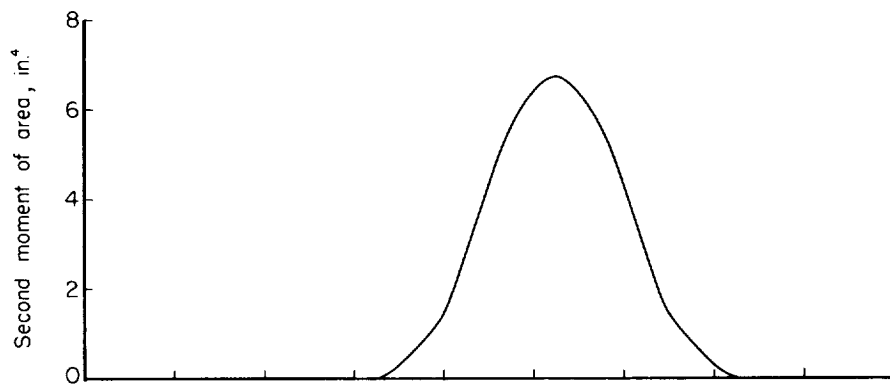


(c) Half moment-of-area-rule modification.

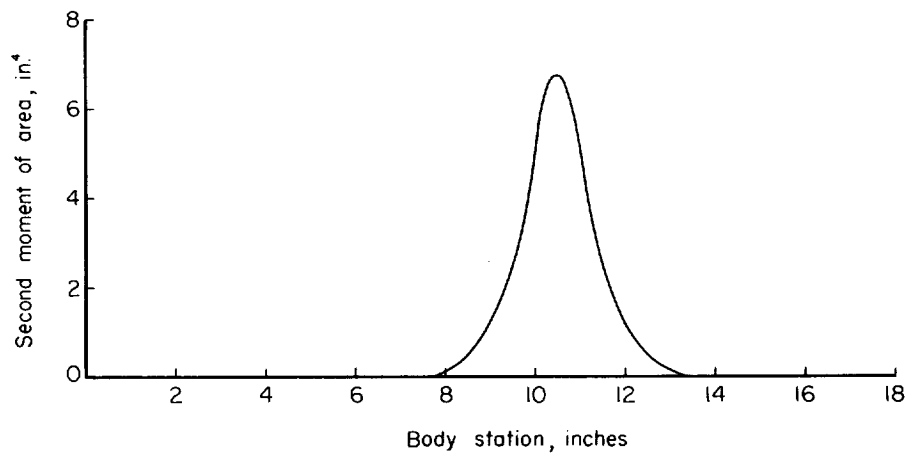
Figure 2.- Longitudinal distributions of cross-sectional area.



(a) Basic wing.

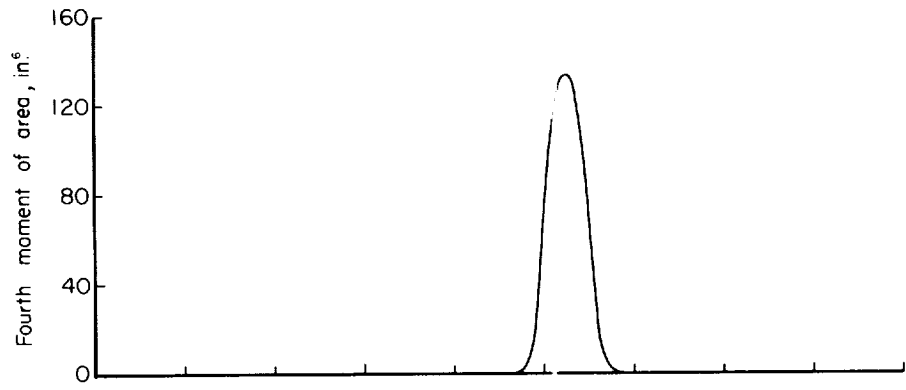


(b) Moment-of-area-rule modification.

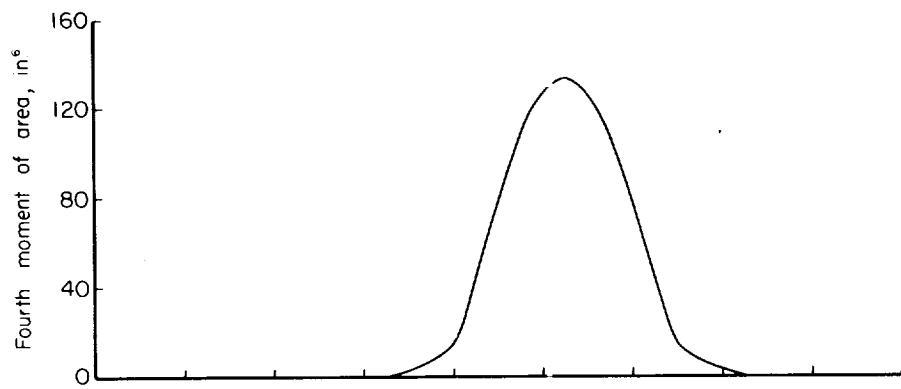


(c) Half moment-of-area-rule modification.

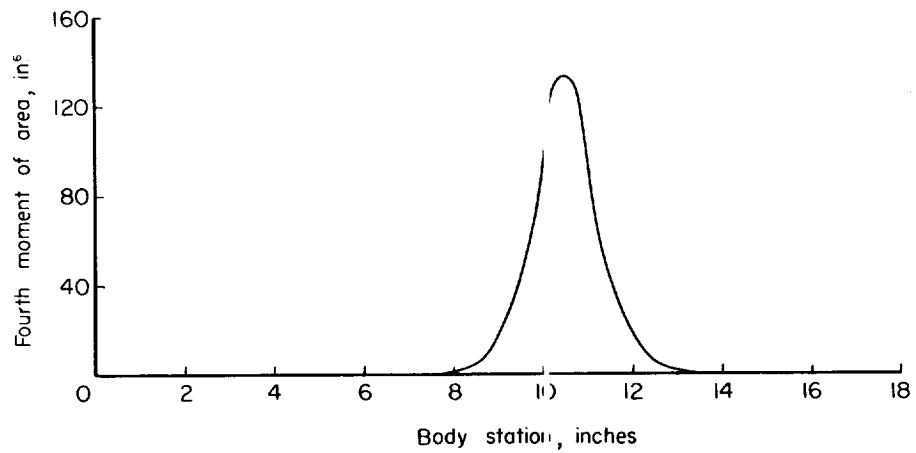
Figure 3.- Longitudinal distributions of the second moment of area.



(a) Basic wing.



(b) Moment-of-area-rule modification.



(c) Half moment-of-area-rule modification.

Figure 4.- Longitudinal distributions of the fourth moment of area.

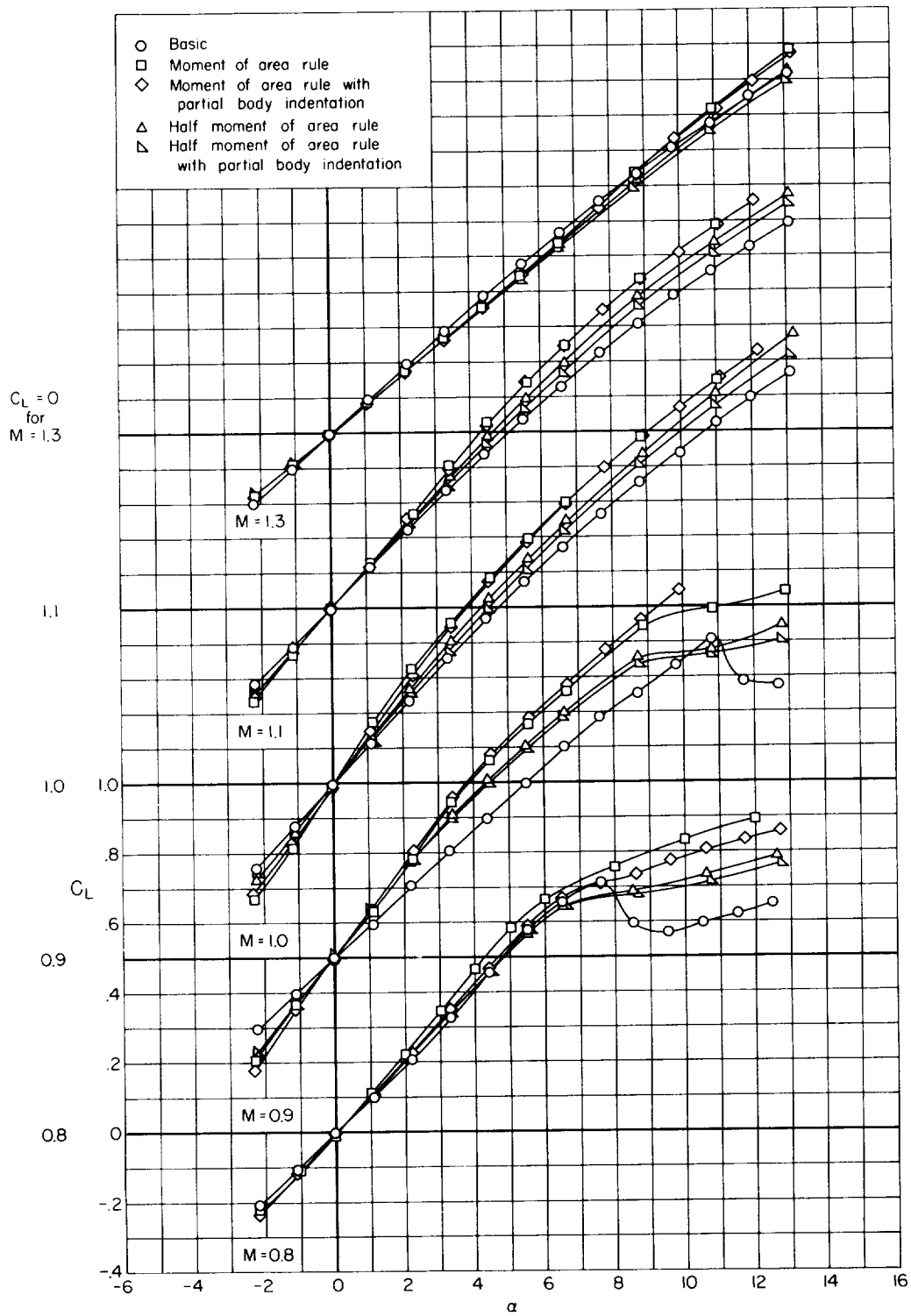


Figure 5.- Variation of lift coefficient with angle of attack.

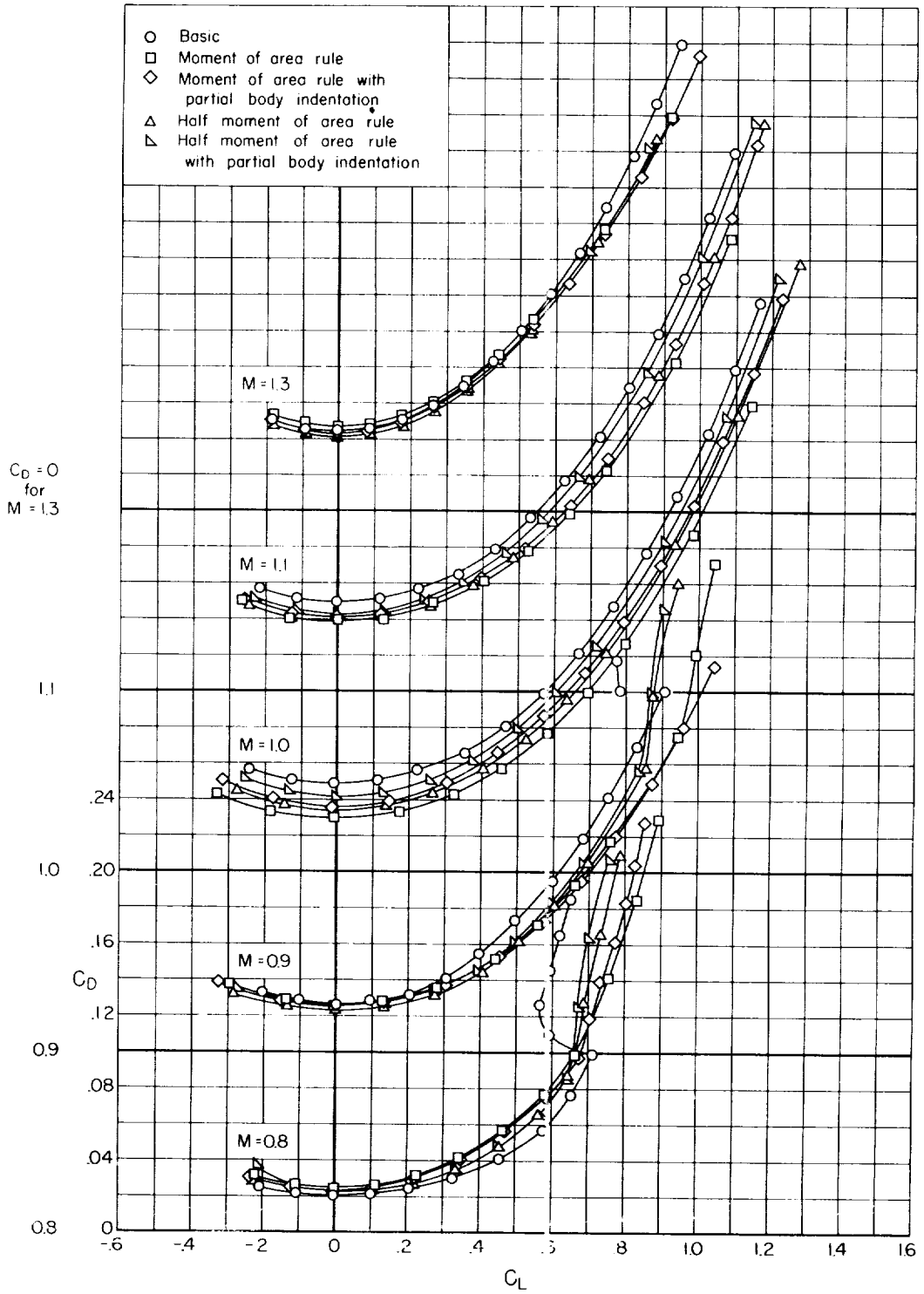


Figure 6.- Variation of drag coefficient with lift coefficient.

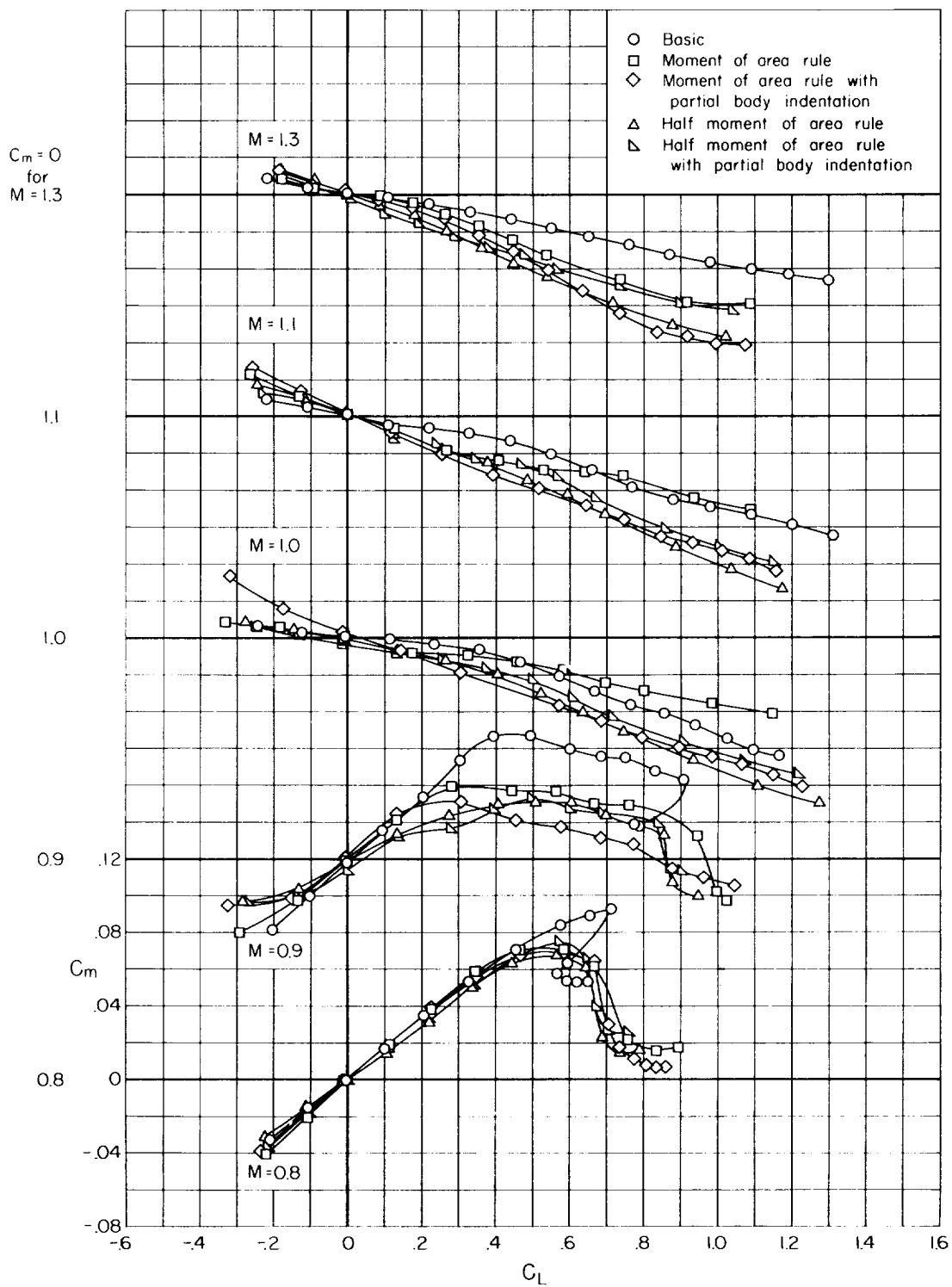


Figure 7.- Variation of pitching-moment coefficient with lift coefficient.

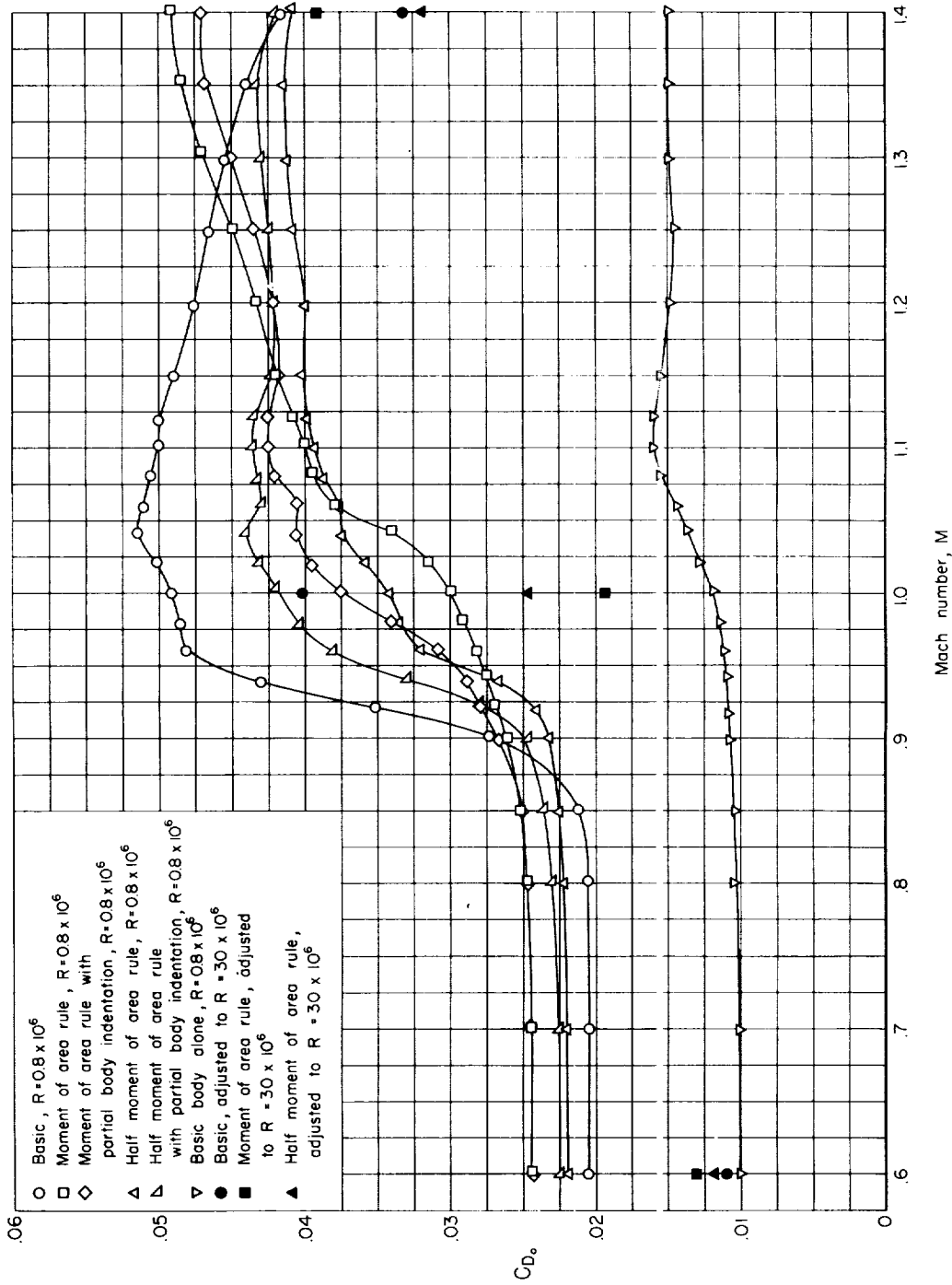


Figure 8.- Variation of zero-lift drag coefficient with Mach number.

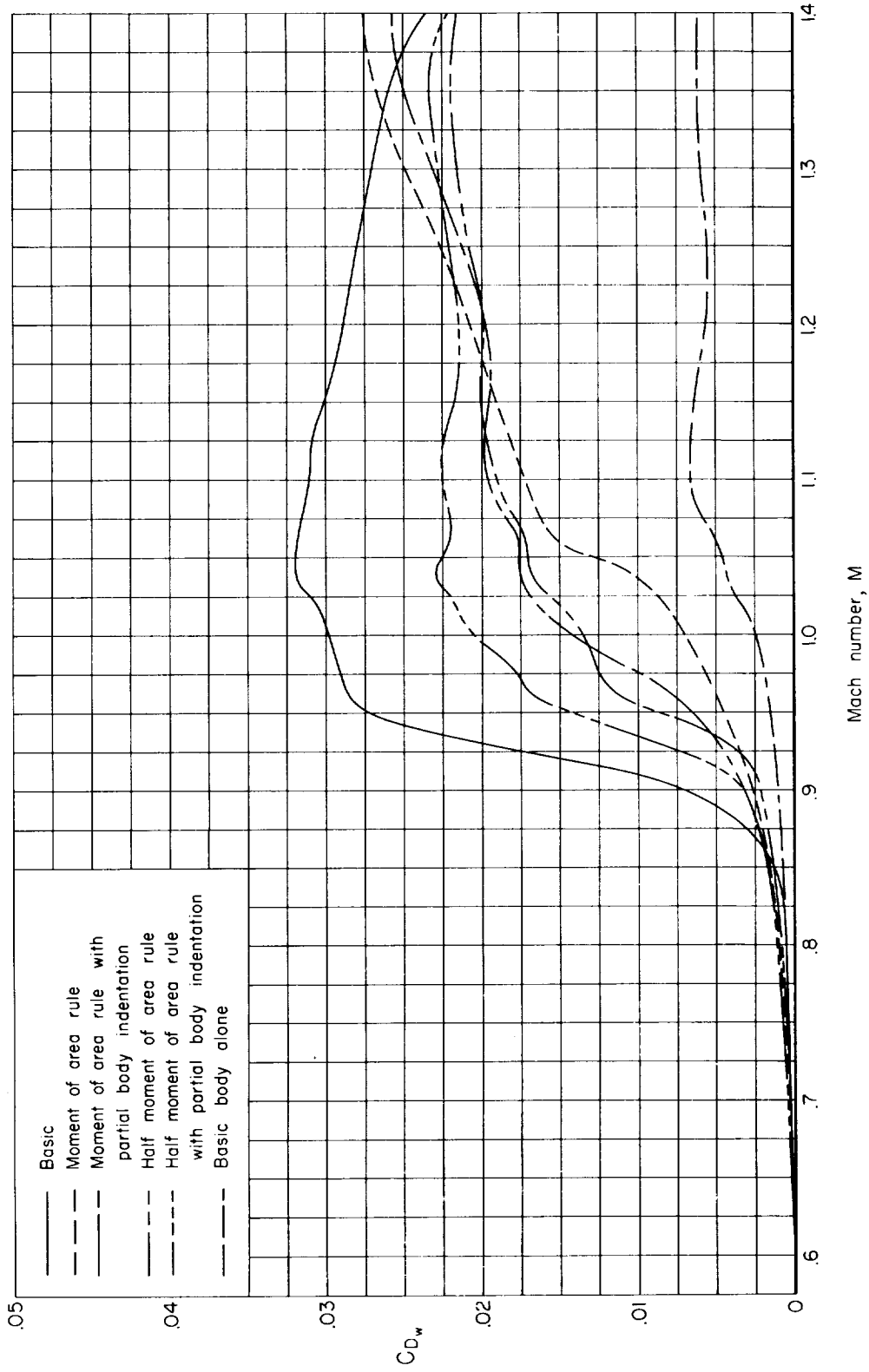


Figure 9.- Variation of wave-drag coefficient with Mach number.

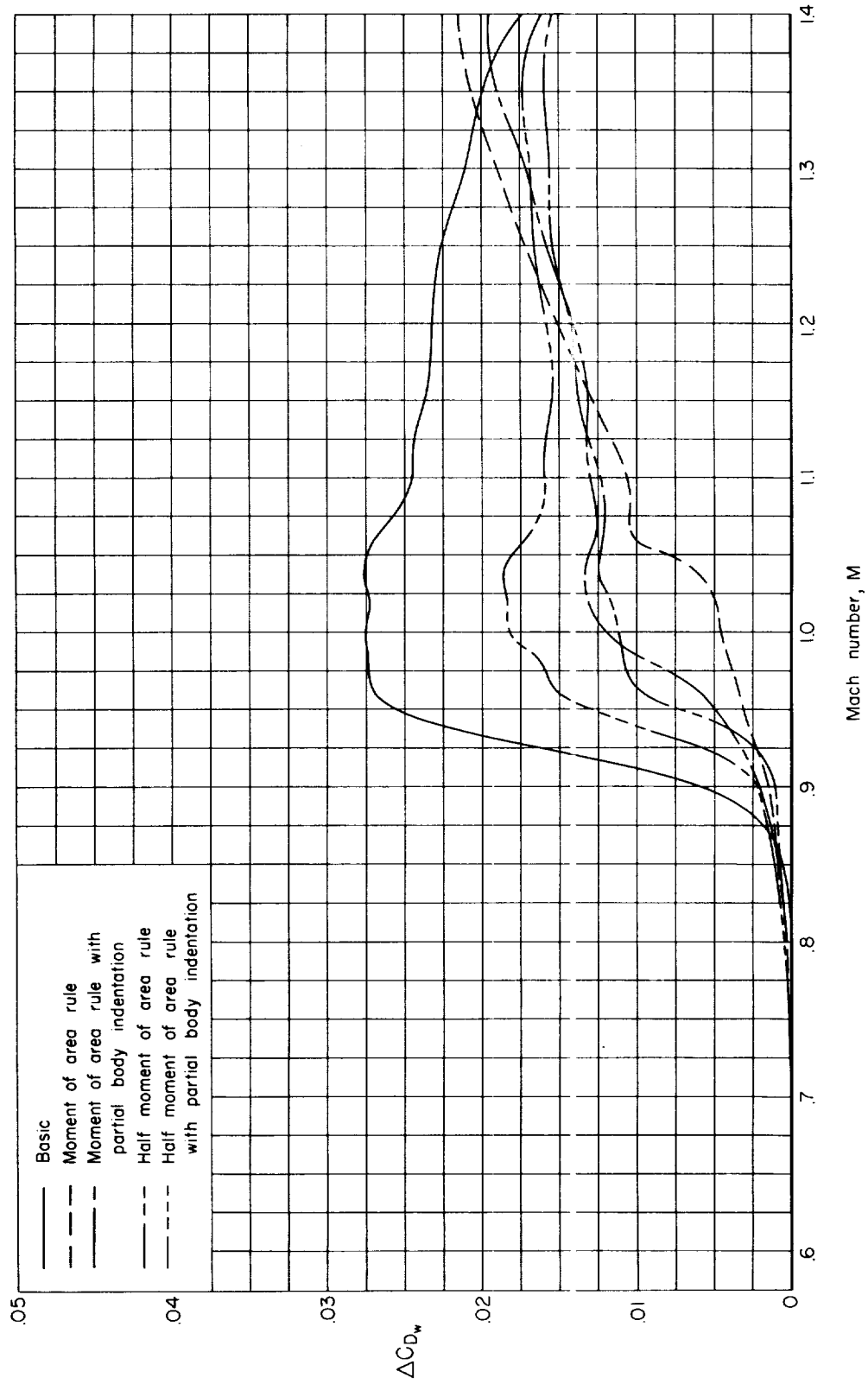


Figure 10.- Variation of incremental wave-drag coefficient with Mach number.

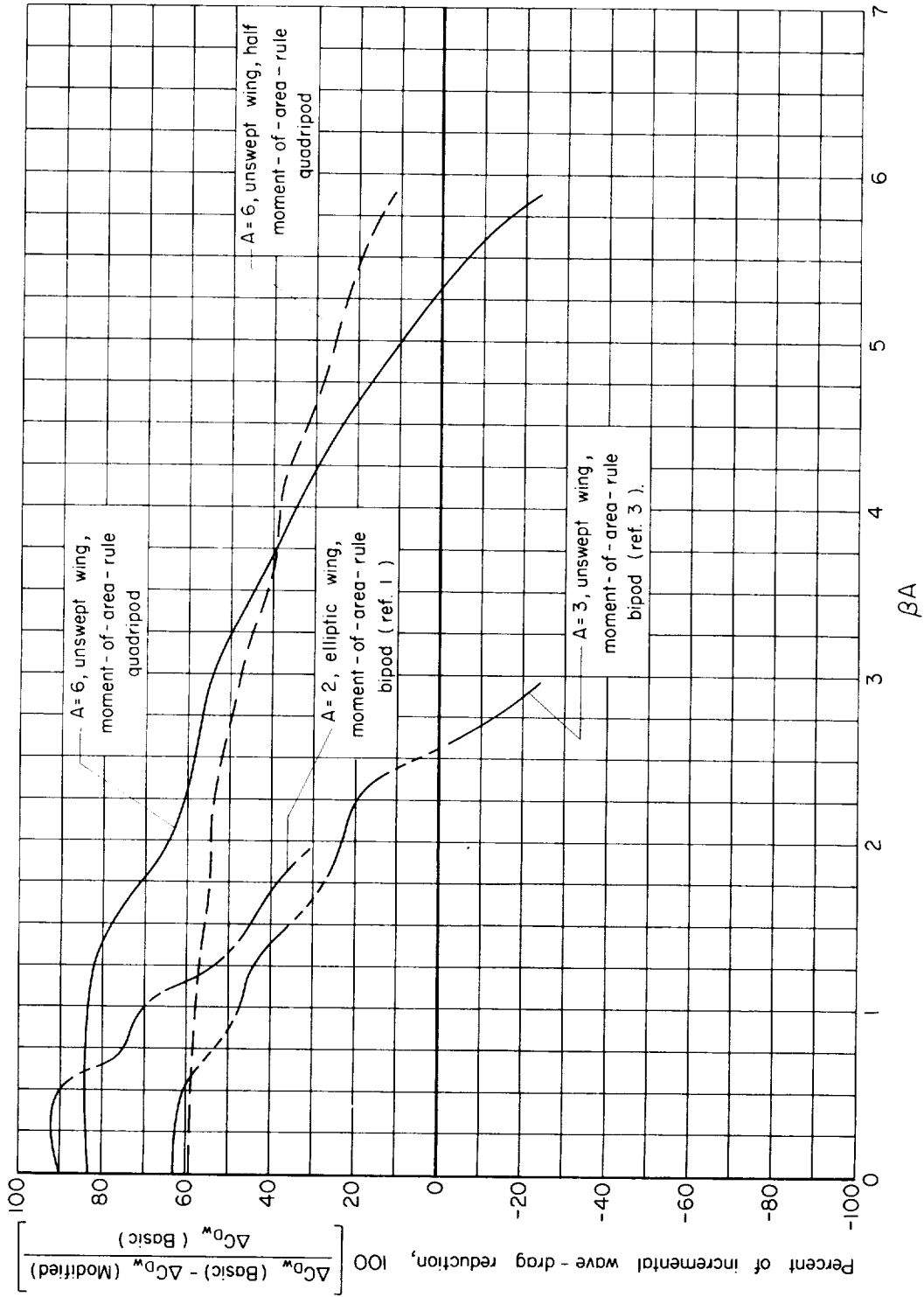


Figure 11.- Variation of incremental wave-drag reduction with reduced aspect ratio.

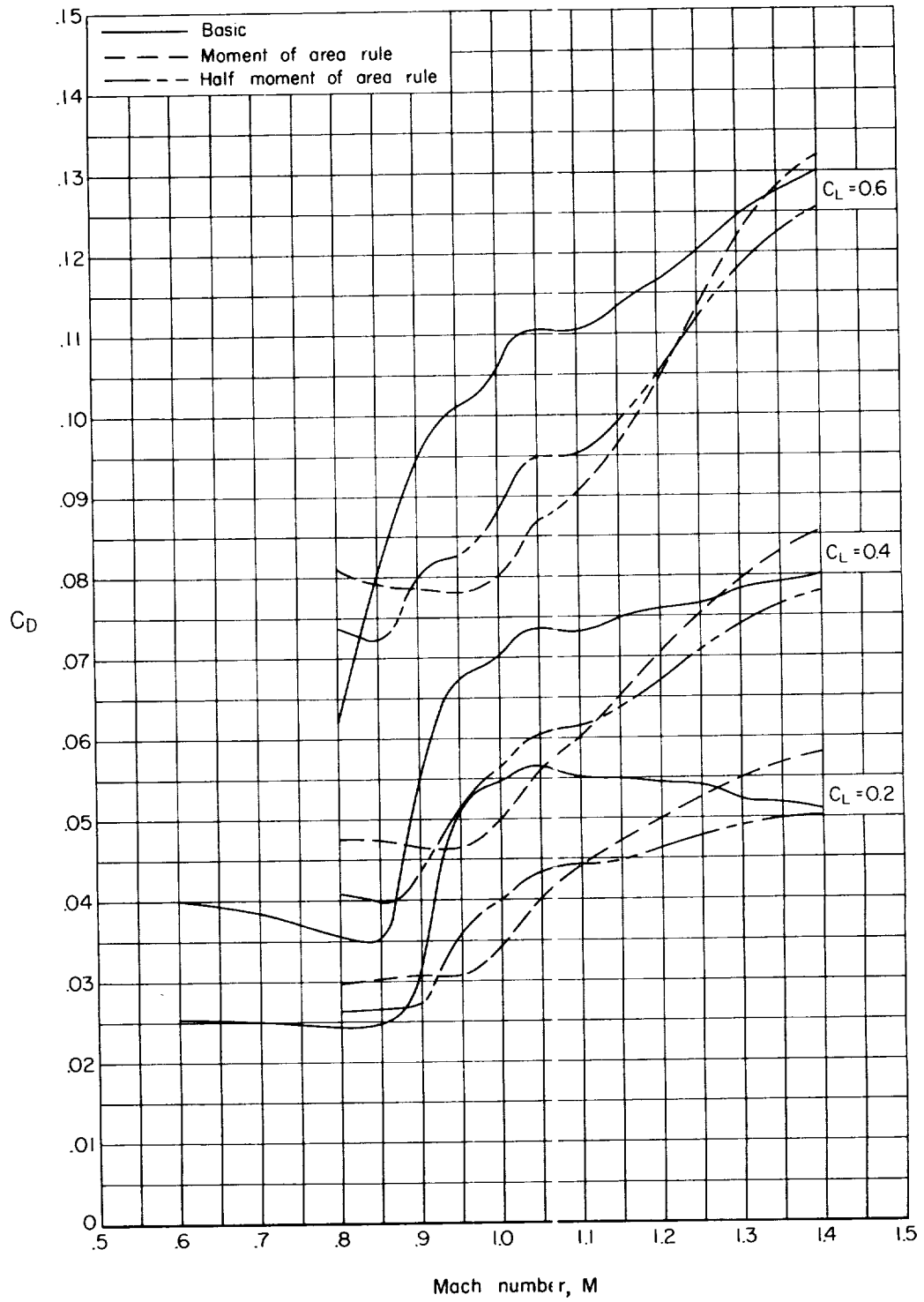


Figure 12.- Variation of drag coefficient with Mach number at lifting conditions.

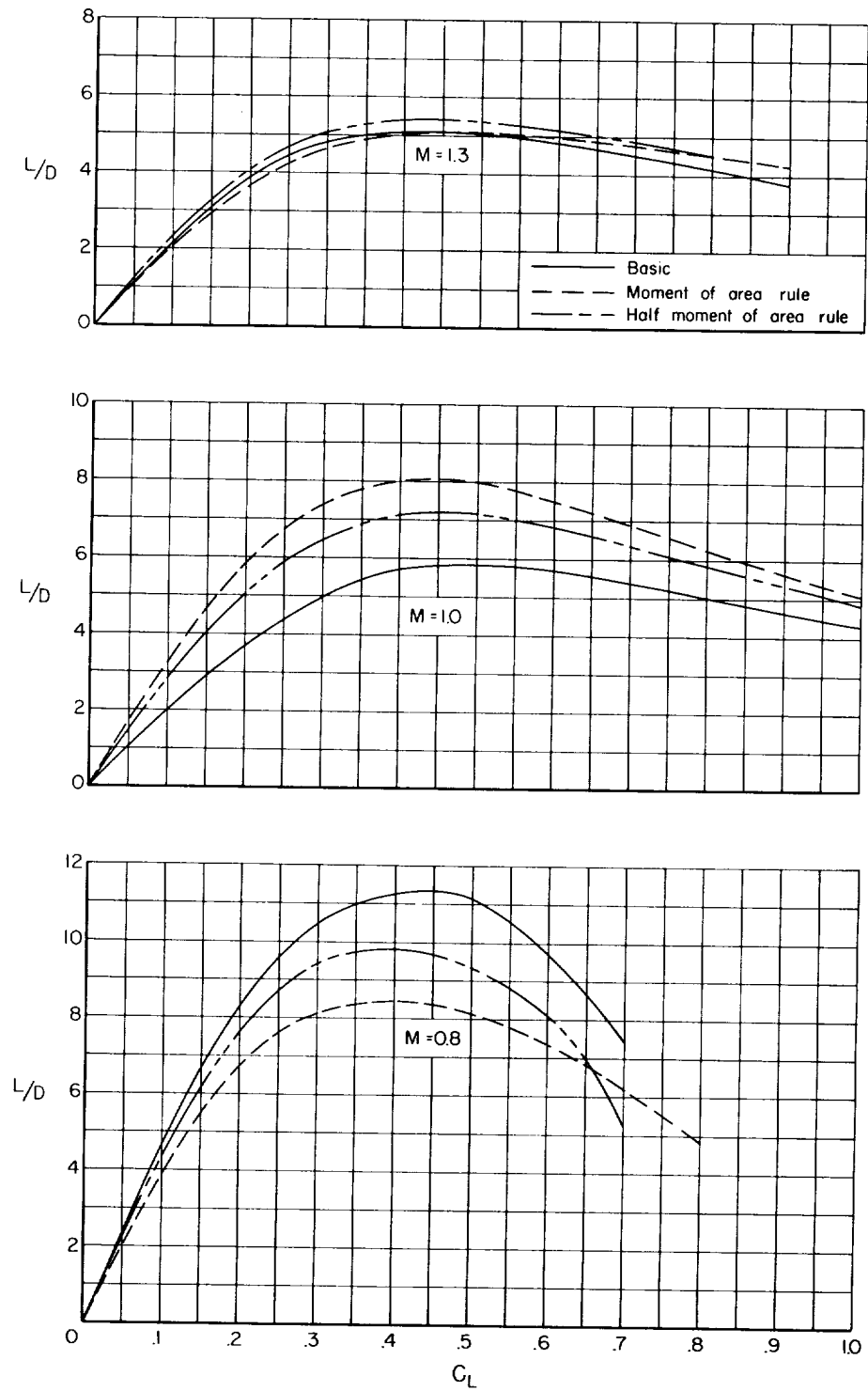


Figure 13.- Variation of lift-drag ratio with lift coefficient.

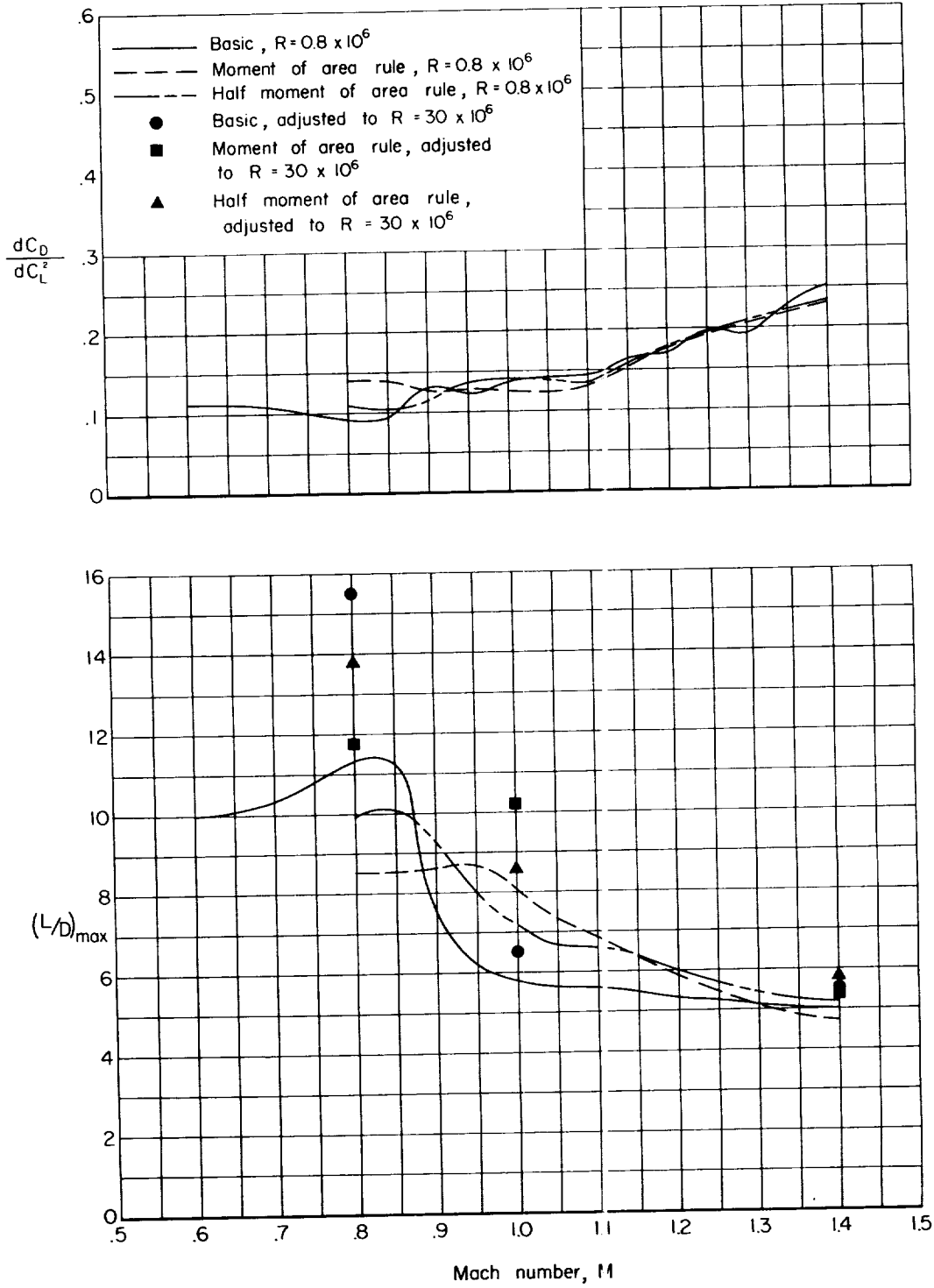


Figure 14.- Variation of drag-rise factor and maximum lift-drag ratio with Mach number.

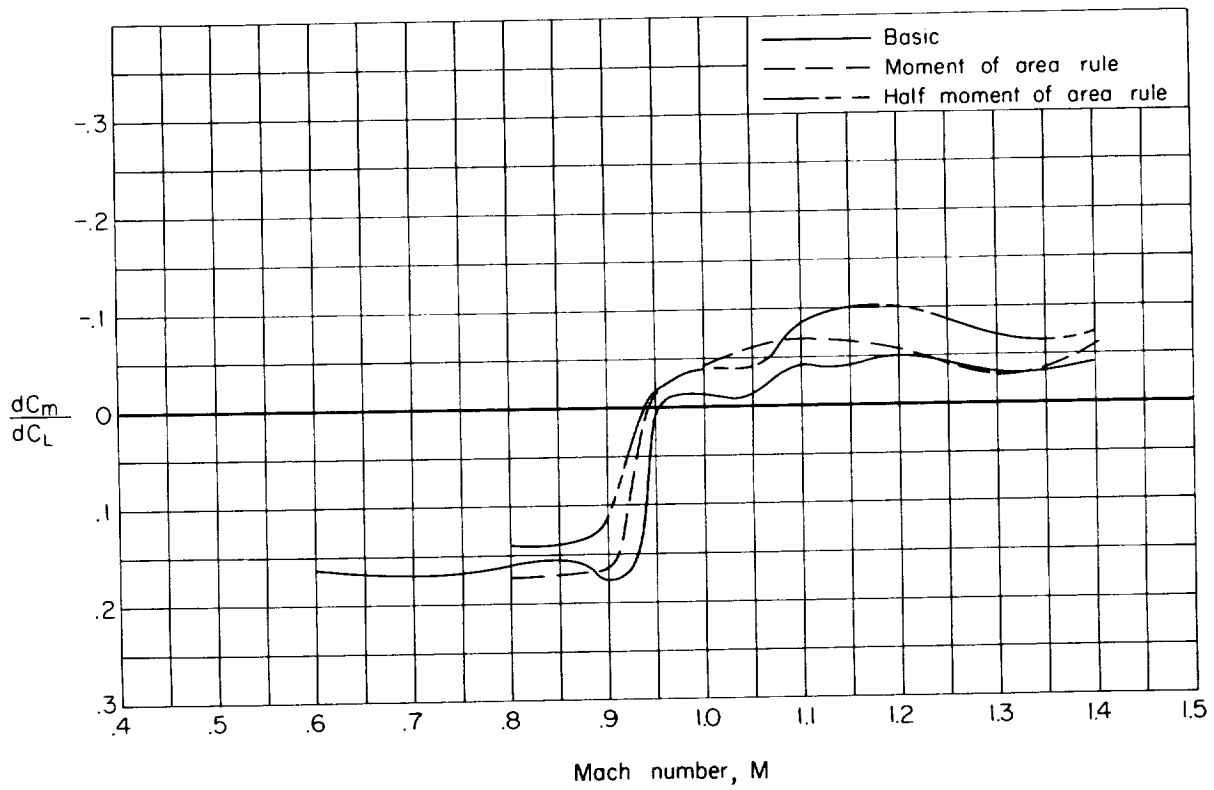
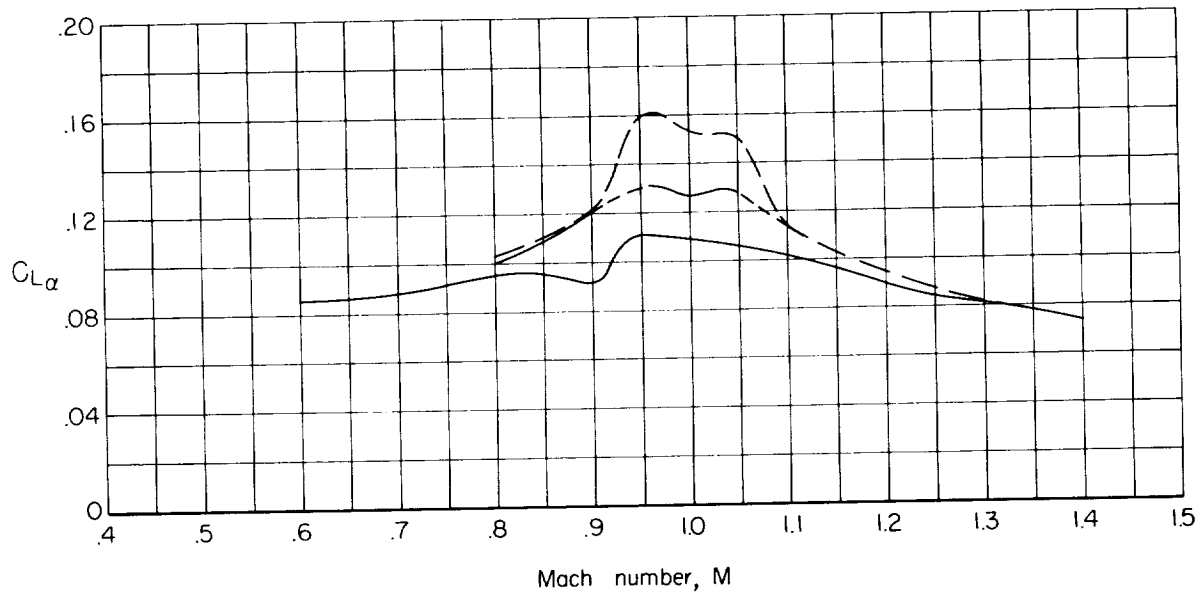


Figure 15.- Variation of lift-curve slope and pitching-moment-curve slope with Mach number.

